Wan Hassan, W. A., Liu, J., Howlin, B. J., Ishida, H., & Hamerton, I. (2016). Examining the Influence of Bisphenol A on the Polymerisation and Network Properties of An Aromatic Benzoxazine. Polymer, 88, 52-62. DOI: 10.1016/j.polymer.2016.01.041

Examining the Influence of Bisphenol A on the Polymerisation and Network Properties of An Aromatic Benzoxazine

Wan Aminah Wan Hassan[#], Jia Liu[‡], Brendan J. Howlin[#], Hatsuo Ishida[‡] and Ian Hamerton[†,*]

[†] The Advanced Composites Centre for Innovation and Science, Department of Aerospace Engineering, University of Bristol, Queen's Building, University Walk, Bristol, BS8 1TR, U.K.

[#]Department of Chemistry, Faculty of Engineering and Physical Sciences, University of Surrey, Guildford, Surrey, GU2 7XH, U.K.

[‡]Department of Macromolecular Science and Engineering, Case Western Reserve University, 10900 Euclid Avenue, Cleveland, Ohio 44106-7202, U.S.A.

*To whom correspondence should be addressed.

ABSTRACT: A series of reactive blends, comprising a commercial benzoxazine monomer, 2,2-*bis*(3,4-dihydro-3-phenyl-2H-1,3-benzoxazine)propane, and bisphenol A is prepared and characterized. Thermal analysis and dynamic rheology reveal how the introduction of up to 15 wt % bisphenol A lead to a significant increase in reactivity (the exothermic peak maximum of thermal polymerization is reduced from 245 ºC to 215 ºC), with a small penalty in glass transition temperature (reduction of 15 K), but similar thermal stability (onset of degradation = 283 ºC, char yield = 26 %). With higher concentrations of bisphenol A (*e.g.* 25 wt %), a significantly more reactive blend is produced (exothermic peak maximum = 192 ºC), but with a significantly lower thermal stability (onset of degradation = 265 ºC, char yield = 22 %) and glass transition temperature (128 ºC). Attempts to produce a cured plaque containing 35 wt % bisphenol A were unsuccessful, due to brittleness. Molecular modelling is used to replicate successfully the glass transition temperatures (measured using thermal analysis) of a range of copolymers.

Keywords: Polybenzoxazines, Bisphenol A, Copolymers, Thermal Behaviour, Molecular Modelling.

INTRODUCTION

Poly(*bis*-benzoxazine)s (sometimes simply referred to as polybenzoxazines) are a family of thermosetting polymers that are obtained through step growth ring-opening polyaddition from *bis*-benzoxazine monomers (Scheme 1), which are in turn the products of the Mannich reaction between a *bis*-phenol, formaldehyde and a primary amine[1]. This, in turn, affects the properties of the resin before, during and after cure (the presence of oligomers bearing hydroxyl groups in the chain is known to enhance the reactivity of the benzoxazine).

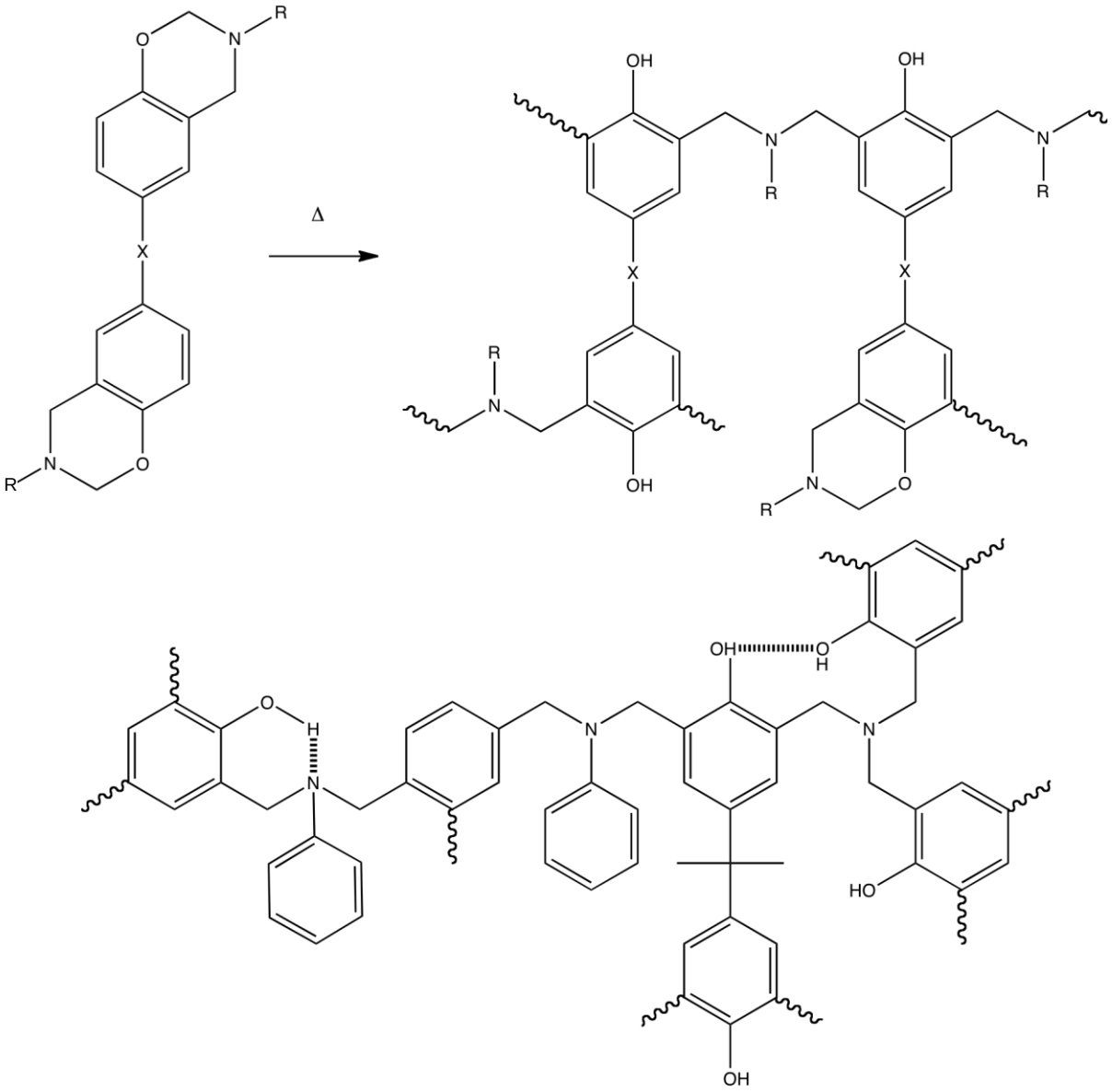

Scheme 1 Schematic showing the polymerisation of bisbenzoxazines through ring opening and crosslinking and representative network.

Commercial benzoxazines, generally in the form of reactive blends with epoxy resins, are currently being evaluated for use in the aerospace industry (in which they would replace or augment phenolic polymers in secondary applications such as interior panelling). Polybenzoxazines appear to incorporate the best properties from conventional phenolics, and may find application in a number of their traditional niches, whilst improving on shelf life and offering the potential for greater toughness properties through their greater molecular flexibility; the relative cheapness of the monomer is also an important factor influencing their adoption. Unlike many other commercial thermosetting resins, which evolve condensation products such as water or ammonia, benzoxazine monomers react relatively cleanly to form a polymer with few reaction by-products[2]. Polymerisation may be effected thermally without the need for initiation, although several catalytic studies have also been conducted[3].

Benzoxazines based on the reaction of bisphenol A (BPA) and aniline date[4] from 1994, and it is arguably the most well established monomer (termed BA-a), having been the subject of almost 100 publications since 1994. The kinetics and mechanism of the monomer to form the homopolymer have been studied in detail using predominantly spectroscopic[5,6,7] and thermal analysis[8,9] techniques. The homopolymer of BA-a offers superior mechanical properties to the corresponding methylamine derivative. For example, the tensile properties (modulus 5.2 GPa, strength 64 MPa) and flexural properties (modulus 4.5 GPa, strength 126 MPa) are superior to typical epoxy resins and phenolics, while the coefficient of thermal expansion (α = 1.7 x 10^4 $cm^3/cm^3.ºC$, β = 58 x 10^6 cm/cm.ºC) and cure shrinkage are both very low (1.9 % at saturation, with a diffusion coefficient of 0.5 x 10^9 cm^2/s)**[10]**. However, toughness of the homopolymer is still a shortcoming (elongation at break 1.3 % and strain at break 2.9 %) and a calculation of crosslink density using Nielsen's equation[11] yields a crosslink density of 1.1 x 10^{-3} mol/cm^3 or 610 Daltons between crosslinks. BA-a also forms the basis of several commercial building blocks, one of which is explored in this work.

Blends of BA-a have been formed with a variety of thermoplastics including polycarbonate[12], poly(ethylene oxide)[13] and latterly ε-caprolactone[14,15,16], in these instances the ability of the blend components to support the formation of hydrogen bonds facilitates improved miscibility, while reaction induced phase separation yields tougher matrices as a result of the new morphologies developed during processing. Reactive blends of BA-a are finding increasing interest in research and the use of epoxy co-monomers[17,18] are pre-eminent, forming the basis of commercial blends such as the Epsilon resins from Henkel[19]; the addition of epoxy improving the processing characteristics of the benzoxazine and related ternary blends have been explored using phenolic co-monomers[20,21,22]. Bisoxazolines are less common in this context[23], although they have a longer history in the modification of phenolics[24], conferring lower heat and smoke release properties. The formation of BA-a nanocomposites based on silica[25] and various silicate clay species[26,27,28,29] has been explored and improvements in thermal and mechanical properties can be realized with comparatively modest loadings. However, the processing procedures required to ensure optimum exfoliation to allow intercalation of the benzoxazine component within the laminae of the clays are not trivial.

The incorporation of BPA serves a secondary function to increase the reactivity of the blend serving as an initiator/co-reactant. Thus, the purpose of this study is to establish structure-property relationships for a series of novel reactive blends comprising the most common and widely studied of the difunctional benzoxazine monomers, based on bisphenol A and aniline, and bisphenol A.

EXPERIMENTAL SECTION

Materials. 2,2-*bis*(3,4-Dihydro-3-phenyl-2H-1,3-benzoxazine)propane (BA-a, as MT35600 *ex* Huntsman) and 2,2-*bis*(3,4-Dihydro-3-phenyl-2H-1,3-benzoxazine)propane (Aldrich, 97 %) were characterized fully using ^{1}H NMR, Raman spectroscopy and elemental analysis and used as received without further purification. In the interests of brevity the characterisation data for the monomer have been deposited as supplementary information.

Blending and cure of samples for analysis.

Four blends were prepared, comprising BA-a and bisphenol A (BPA) in varying ratios (Table 1) using the same method in each case.

Table 1. Blends prepared for analysis in this work

Sample	**BA-a /g (mol.)**	**Bisphenol A /g (mol.)**
BA-a	5.00 (1.1×10^{-2})	-
BA-a/$BPA_{5\%}$	4.75 (1.0×10^{-2})	0.25 (1.1×10^{-3})
BA-a/$BPA_{15\%}$	4.25 (9.2×10^{-3})	0.75 (3.3×10^{-3})
BA-a/$BPA_{25\%}$	3.75 (8.1×10^{-3})	1.25 (5.5×10^{-3})
BA-a/$BPA_{35\%}$	3.25 (7.0×10^{-3})	1.75 (7.7×10^{-3})

Both BA-a and BPA were heated until molten (on a thermostatted hot plate/stirrer) and BPA was added to BA-a, (maintained at 70-80 ºC). The resulting mixture was stirred until homogeneous and cooled before being ground in a mortar with a pestle, to achieve a powder (Table. 1, see supplementary Fig. S1). Samples for thermal analysis were degassed in a vacuum oven (100 °C, 1 hour + 120 °C, 1 hour). If the samples were to be cured for submission in dynamic mechanical thermal analysis, then the degassed blends were cured (180 ºC, 2 hours) then the oven was switched off and allowed to cool, with the samples within, overnight.

Instrumentation. Nuclear magnetic resonance (NMR) spectra were obtained for ^{1}H (500 MHz) and ^{13}C (125.721 MHz) using a Bruker DRX500 FT-NMR at 298K in $CDCl_3$ with TMS.

Infra-red spectra were obtained (32 scans between 4000-600 cm^{-1}) using an Agilent Technologies Cary 600 Series Fourier Transform Infrared spectrometer employing a golden gate accessory with a

diamond crystal was used for all ATR-IR spectroscopy analyses. Spectra were obtained at a resolution of 4 cm^{-1} and co-added to produce the final spectrum. Principal components analysis (PCA) was performed using Unscrambler X software[30] v.10.1.

Raman spectra were obtained using a Perkin-Elmer system 2000 FT-NIR-Raman spectrometer operating at 250-500 mW (Nd-YAG laser).

Differential scanning calorimetry (DSC) was undertaken using a TA Instruments Q1000 running TA Q Series Advantage software on samples (5.5 ± 0.5 mg) in hermetically sealed aluminium pans. Experiments were conducted at a heating rate of 10 K/min. from room temperature to 300 °C (heat/cool/heat) under flowing nitrogen (50 cm^3/min.), then cooled to room temperature at 10 K/min. The T_g was determined from the midpoint of the inflexion in the heat flow curve during both the cooling step and the re-scan (heating) experiment.

Thermogravimetric analysis (TGA) was performed on a TA Instruments Q500 on cured particulate resin samples and small sections of composite (6.5 ± 0.5 mg) in a platinum crucible from 20-800 °C at 10 K/min in nitrogen (60 cm^3/min).

Dynamic mechanical thermal analysis (DMTA) was carried out in single cantilever mode at a frequency of 1 Hz (0.1 % strain) on cured neat resin samples (2 mm x 15 mm x 35 mm) using a TA Instruments Q800. Samples were heated from 20-250 °C at 10 K/min in static air.

Rheological analysis was performed at Case Western Reserve University using a Rheoplus instrument using v.3.40 software. Samples were oscillated with 10 % strain and an angular frequency omega of 10 rad/s at a temperature of 180 °C.

Methodology for Molecular Modelling. The molecular modelling program Accelrys Materials Studio[31] version 6.0 was utilised within this work and all the modelling work was carried out using an in house PC. The potential energy for all models throughout this work was calculated using the Condensed-phase Optimised Molecular Potential for Atomistic Simulation Studies (COMPASS)[32], a force field specifically designed for polymer calculations. Molecular models were all created using a combination of the Materials Studio[31] modules and in-house programs to simulate cure. Initially, the structure of the polybenzoxazine, poly(BA-a), was simulated at zero Kelvin using molecular mechanics (MM)[33]. To optimise the structure of the molecule, the steepest-descents, conjugate gradients and Newtonian[34] methods were performed to minimise the energy of the molecule. This yielded bond lengths that agreed well with published crystallographic data (Table 2) for similar monomers or compounds[35]. The Materials Studio Visualiser was used to create 3D models of the monomers and impurities, which were then packed into a periodic cell, which was repeated in 3D

space with voidless packing. The benzoxazine monomers were ‘cured’ *in silico* using a cure program from 0 °C to 300 °C to effect crosslinking. Cut-off distances of 0.5 nm and 0.6 nm were used in parallel experiments generating network models. Each model was subjected to molecular dynamics (MD) simulation by raising the temperature (*in silico*) in 10 K increments from 273 K to 573 K and saving the trajectory files.

Table 2 Selected bond distance and angles for BA-a obtained using the Dreiding forcefield (for given conformation) compared with empirical x-ray data[36]

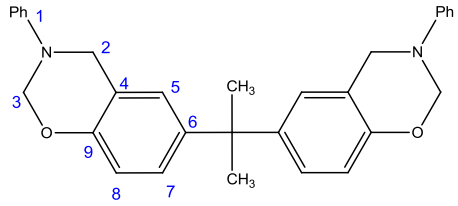

Bond lengths (nm)				Bond angles (°)				Dihedral angle (°)			
	Modelling data (0.5 nm)	**Modelling data (0.6 nm)**	**Empirical data[35]**		**Modelling data (0.5 nm)**	**Modelling data (0.6 nm)**	**Empirical data[35]**		**Modelling data (0.5 nm)**	**Modelling data (0.6 nm)**	**Modelling data[36]**
C9-O	1.40	1.39	1.36	C9-O-C3	117.5	115.8	119.9	C4-C9-O-C3	21.6	10.8	13.4
O-C3	1.44	1.43	1.45	O-C3-N	114.8	113.6	113.5	C3-N-C2-C4	63.6	-53.9	-49.8
C3-N	1.47	1.48	1.43	C3-N-C2	112.3	108.6	107.9	C9-O-C3-N	0.6	-40.7	-43.8
N-C2	1.47	1.47	1.47	N-C2-C4	103.8	108.2	110.2	C9-C4-C2-N	-42.5	27.2	22.3
C2-C4	1.50	1.52	1.51	C2-C4-C9	118.8	121.7	117.7	O-C3-N-C2	-45.5	64.4	62.7
N-C1	1.43	1.43	-	C4-C9-O	120.4	120.5	123.1	O-C3-N-C1	-176.4	-165.1	-62.6
C9-C4	1.40	1.40	1.39	C3-N-C1	112.6	112.7	-				

RESULTS AND DISCUSSION

The cured binary blends (Fig. 1, see supplementary Fig. S2 for coloured images) were homogeneous, and were removed carefully from the aluminium moulds, all remained intact with the exception of BA-a/$BPA_{35\%}$, which cracked repeatedly. Although the latter was analysed using several techniques, it was deemed too brittle for measurement using DMTA. The poor fracture toughness of cured neat polybenzoxazines lies at the heart of many studies and BA-a has been blended with reactive rubber species[37,38] to improve their fracture properties, but there is some penalty to be paid in T_g. Core shell rubber technology offers another route to improving toughness, without the same detrimental effect on T_g, which and recent work[39] has shown significant improvements in tensile behaviour (an improvement of 32 % in strain at break), although at higher loadings (16-32 wt %) the tensile strength and Young's modulus suffer. However, a simpler approach to impart greater toughness and modify the polymer network is to increase the molecular weight or rotational freedom between crosslinks and this is explored here.

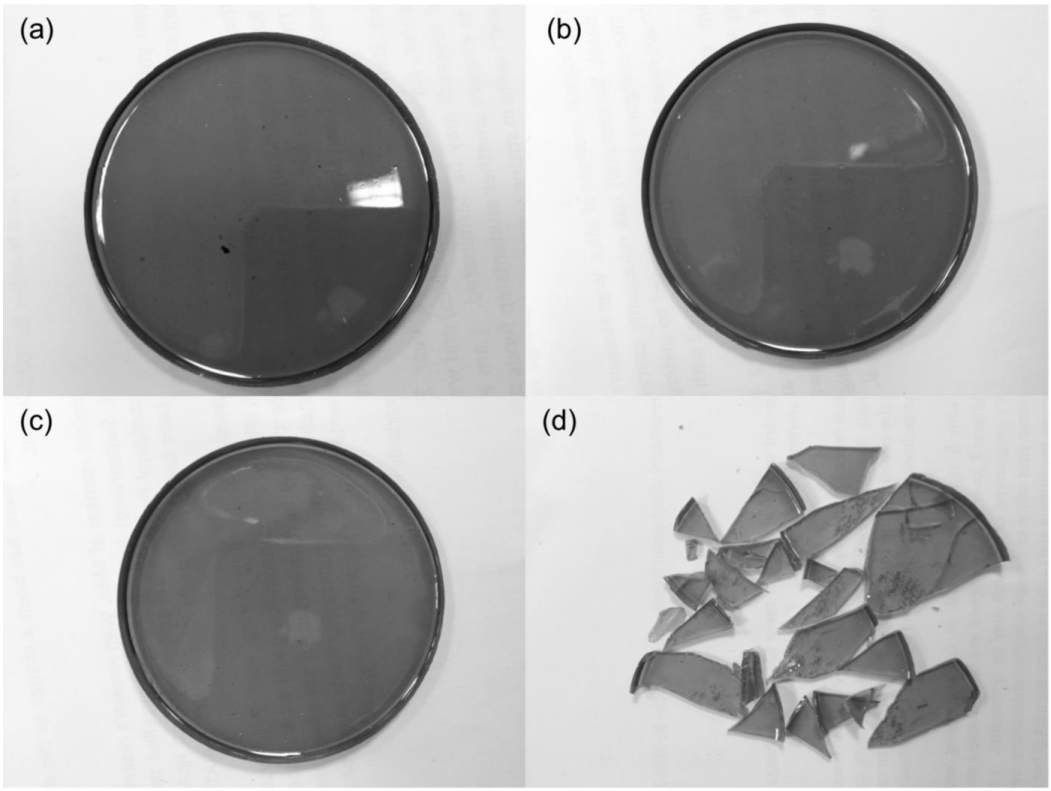

Fig. 1 Images of cured, blended samples of poly(BA-a) containing (a) 0 wt %, (b) 5 wt %, (c) 25 wt %, (d) 35 wt % BPA (following removal from the aluminium pans).

Analysis of the reactivity of the uncured blends and spectral analysis of the cured blends. The cured samples (with the exception of BA-a/$BPA_{35\%}$) were each examined using vibrational spectroscopy and the spectra (Fig. 2) are shown normalized to the 883 cm^{-1} band (an invariant C-H out of plane bend).

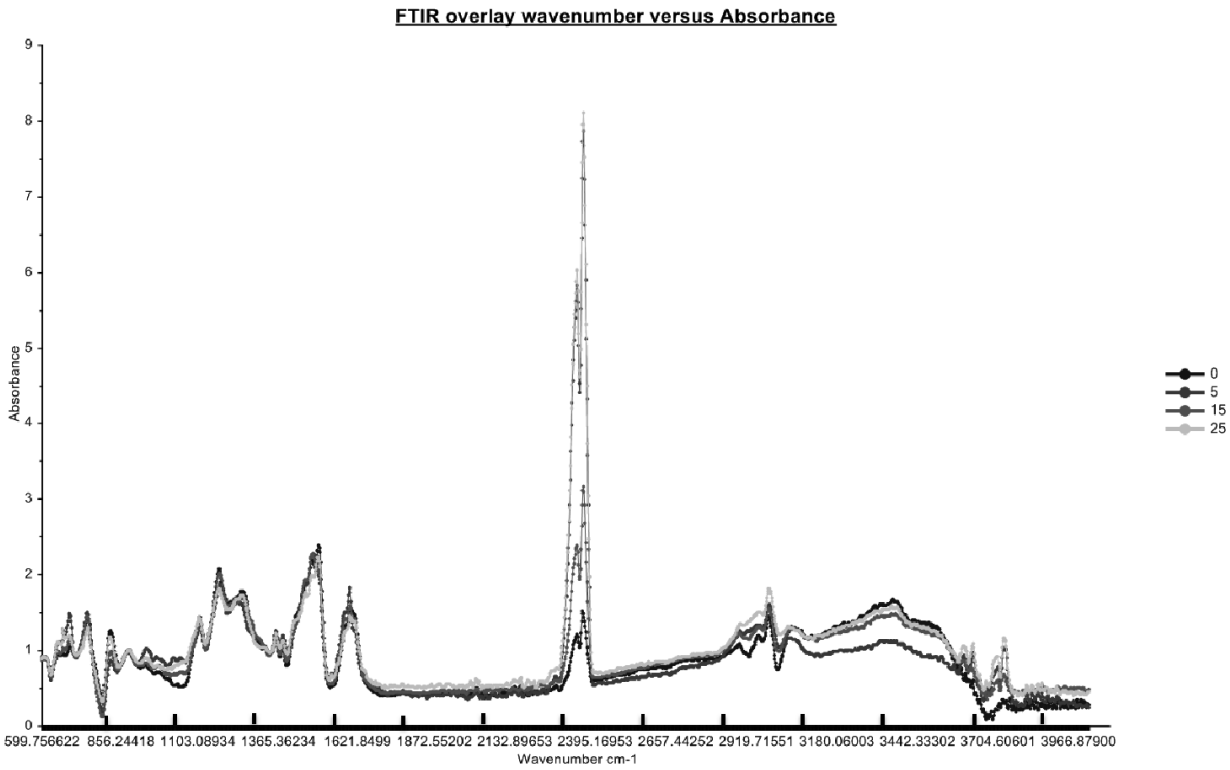

Fig. 2 FTIR data (normalised to 883 cm^{-1}) for various BA-a blends with bisphenol A (0-25 wt %)

PCA was performed on the spectral data for the cured blends, despite the data being small and thus the variables restricted to only four samples. Nevertheless some useful inferences could be made. Fig. 3a shows the scores plot of PC-1 (accounting for 98 % of the data) and PC-2 (accounting for 1 %). It is apparent that wavenumbers comprising PC-1 are centred around 1100-1600 cm^{-1} (C-N, C-O, aromatic C-C stretching and N-H bending); PC2 around 2850-3300 cm^{-1} (C-H, O-H, N-H stretching). The corresponding loadings plots for the two PCs are shown in Fig. 3b and Fig 3c. The score plot shows that poly(BA-a) displays the highest contribution of PC-1 and practically no PC-2; as the BPA content in the cured polymer increases the PC-1 content falls and the PC-2 content grows. Interestingly, while poly(BA-a-*co*-$BPA_{15\%}$) and poly(BA-a-*co*-$BPA_{25\%}$) occupy a similar space and share similar spectra, poly(BA-a-*co*-$BPA_{5\%}$) differs significantly. This suggests the prevalence of a different cured polymer network (perhaps relating to the co-reaction mechanism) as the BPA content increases.

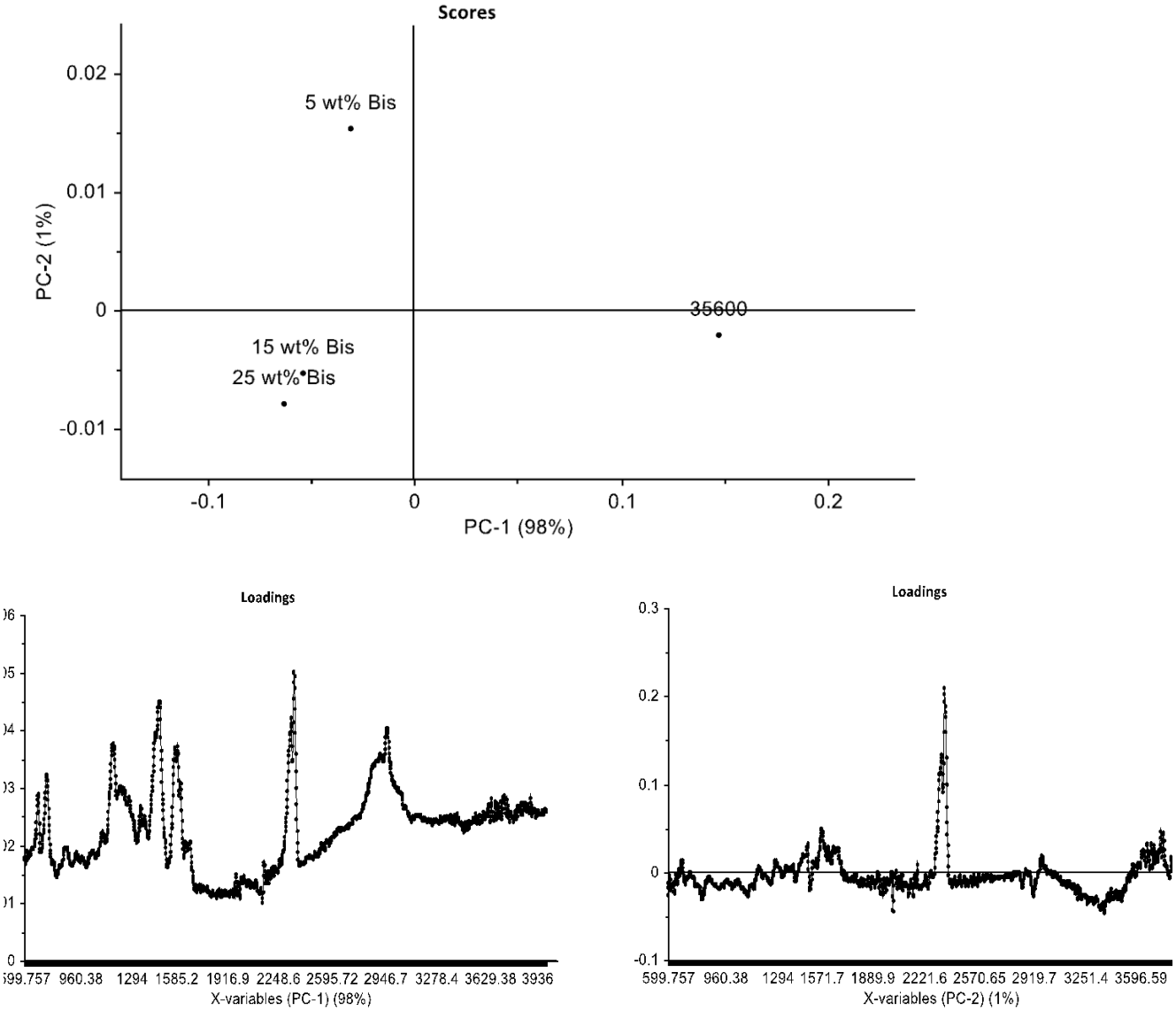

Fig. 3 Scores plots for PC-1 and PC-2 for cured poly(BA-a) blends containing various concentrations of BPA (top) and loadings lots for PC-1 (bottom left) and PC-2 (bottom right).

In a previous publication, we examined the acceleration of the ring opening reaction of the BA-a monomer using active hydrogen donors[40], such as thiodiphenol (1-25 mol%). The DSC profile recorded for the blend of BA-a containing 25 wt% BPA in this work is similar to the profile of the BA-a containing 12 mol% thiodiphenol. In the latter the initial stages of reaction were drawn out, so that several consecutive reactions occur: *i.e.*, the first (and smaller second) peak was associated with ring-opening; the third peak, which accounted for the bulk of the reaction, was attributed with bridge forming, and the last peak to structural rearrangement or possible beginnings of degradation.

The polymerisation behaviour of the blends was examined using DSC and the characteristics are given in Table 3. The analyses were generally very reproducible as evidenced by the thermograms (Fig. 4). Evidently as the BPA content is increased not only does the initial stage of the

polymerisation exotherm move to a lower temperature regime (the initial ring opening is known to be accelerated by active hydrogen donors[40], but the breadth of the exotherm grows to reveal an increasingly complex peak comprising at least three processes.

Table 3 DSC data for cure of BA-a at 10 K/min, under nitrogen (mean values given in italics)

Sample	T_{onset} (ºC)	T_{max} (ºC)	ΔH_p		T_g (ºC)
			(J/g)	(kJ/mole Bz)	
BA-a	213	245	324.9	75.2	162
	212	245	315.7	73.0	157
	211	245	325.3	75.2	153
Mean	*212*	*245*	*322*	*74.5*	*157*
BA-a/$BPA_{5\%}$	183	230	346.2	76.1	146
	179	229	317.5	69.8	149
	177	229	334.9	77.5	145
Mean	*180*	*229*	*333*	*74.5*	*147*
BA-a/$BPA_{15\%}$	163	215	350.0	68.8	143
	161	214	361.3	71.0	143
	164	215	336.1	66.1	144
Mean	*163*	*215*	*349.1*	*68.6*	*143*
BA-a/$BPA_{25\%}$	120	192	340.7	59.1	119
	122	193	336.4	58.4	128
	125	192	344.8	59.8	129
Mean	*122*	*192*	*340.6*	*59.1*	*125*

Key

T_{onset} = Initial temperature of polymerisation exotherm.

T_{max} = Temperature of maximum of polymerisation exotherm.

ΔH_p = Enthalpy of polymerisation,

T_g = Glass transition temperature.

=

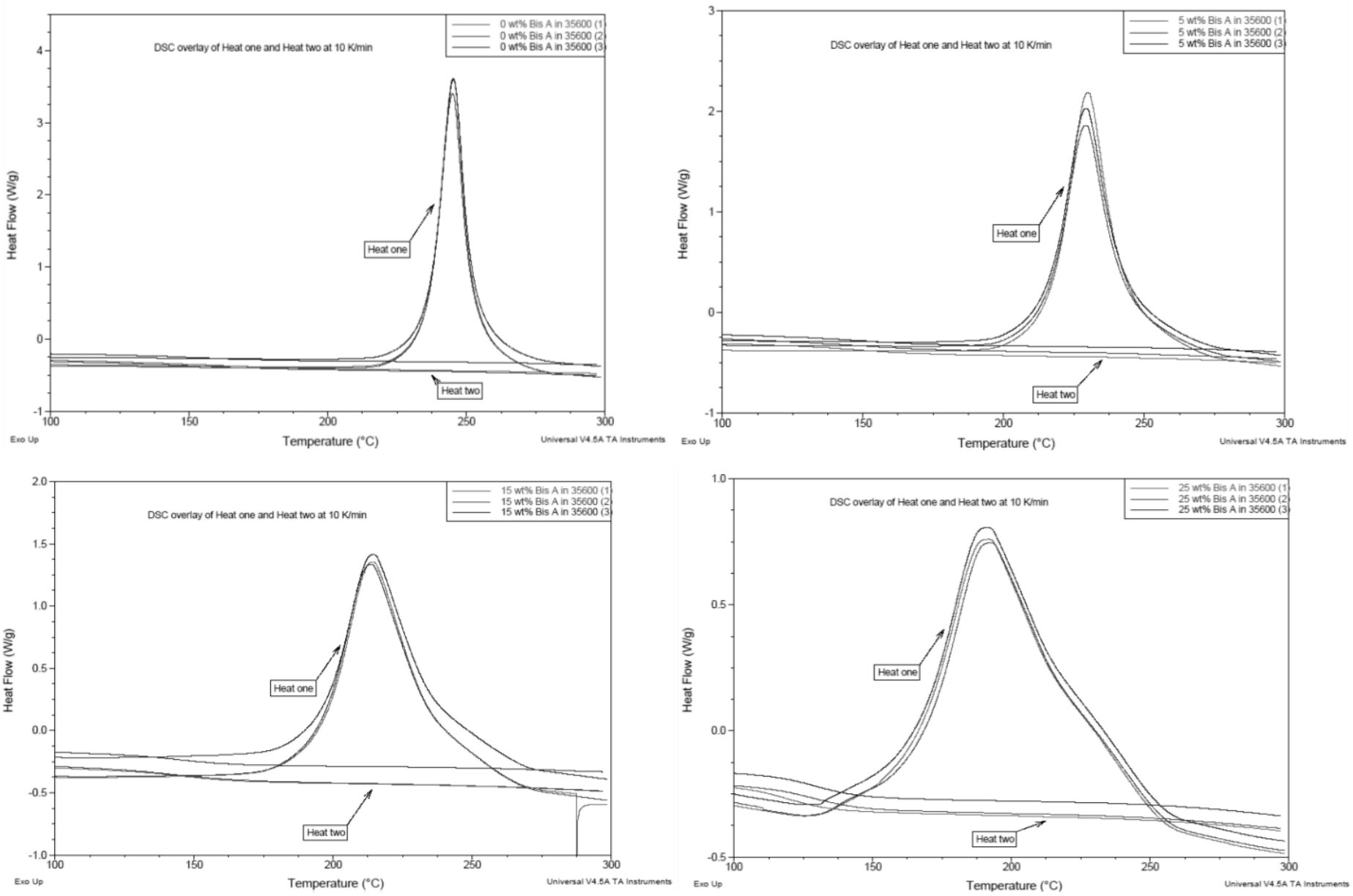

Fig. 4 DSC overlay for first and second heating scans for BA-a containing different concentrations of bisphenol A.

Rheological analysis was also performed on the uncured blends in parallel with the DSC measurements. In the dynamic rheology analysis, the gel point is determined from the intersection of the G' (storage modulus) and G" (loss modulus) (Fig. 5). Thus, at an isothermal cure temperature of 180 °C (mimicking the cure schedule employed) the BA-a is the least reactive of the compounds (gel point *ca.* 2300 seconds). As the BPA content is increased the gel point drops progressively, reaching *ca.* 250 seconds for BA-a/$BPA_{15\%}$, but so reactive is the highest bend (BA-a/$BPA_{25\%}$) that it had undergone gelation before the rheometer had reached the analysis temperature. This finding is consistent with the DSC data (Fig. 4) wherein at 10 K/min BA-a/$BPA_{25\%}$ had undergone a significant degree of cure (> 50 %) by 200 °C.

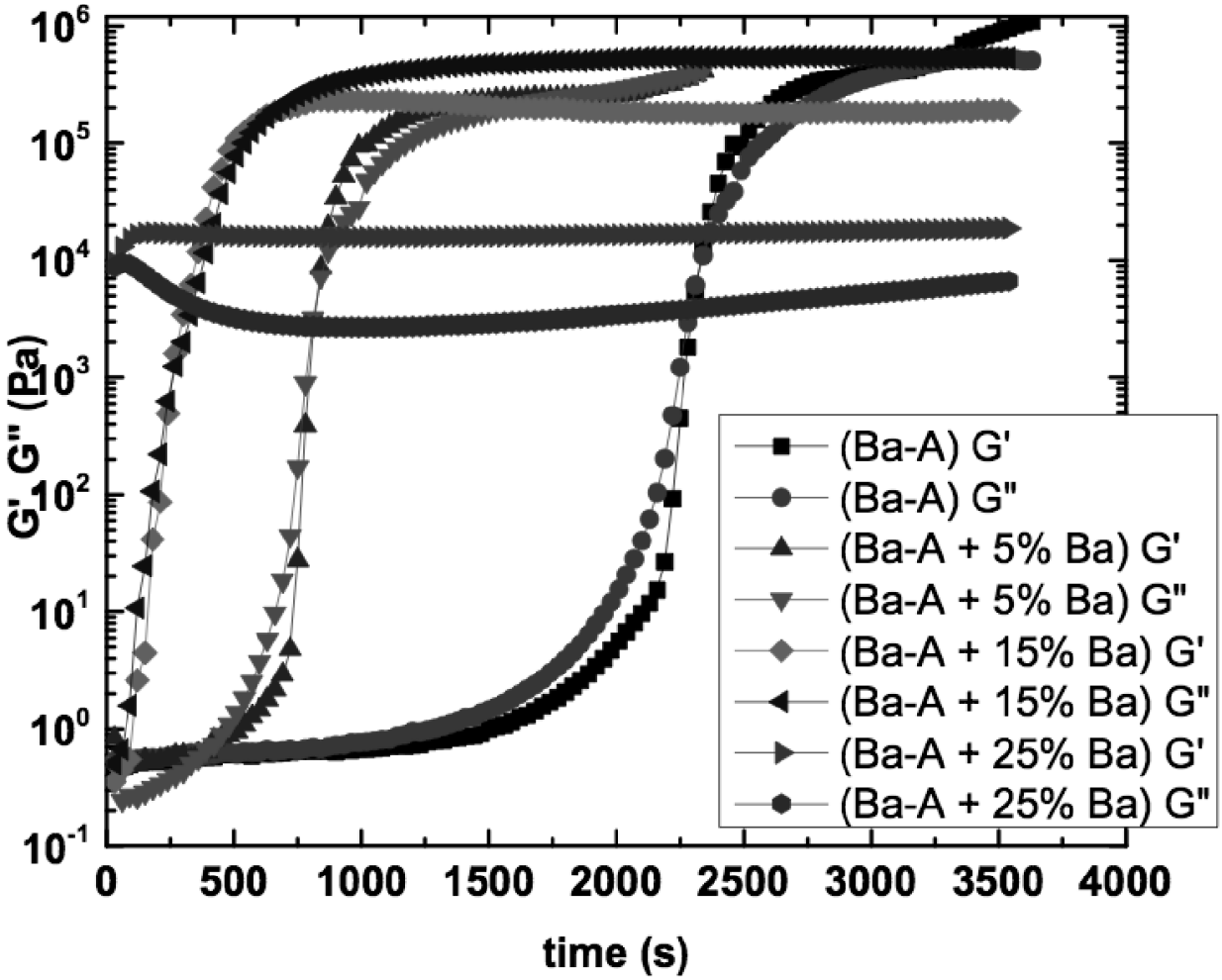

Fig. 5 Rheological characteristics (time sweep at 180 °C) of BA-a containing different quantities of BPA.

Determination of the thermal stability of the polybenzoxazines and relation to structure. During the DSC analysis the second heating scan (of the cured polymers) revealed the presence of the T_g for each network (Table 4) as a discontinuity in the baseline due to the change in heat

capacity experienced by the cured polymer. However, the T_g values revealed by DSC are broad and occur over a comparatively wide range of temperatures (Fig. 6), consequently parallel measurements were made using DMTA on cured resin blends (Fig. 7).

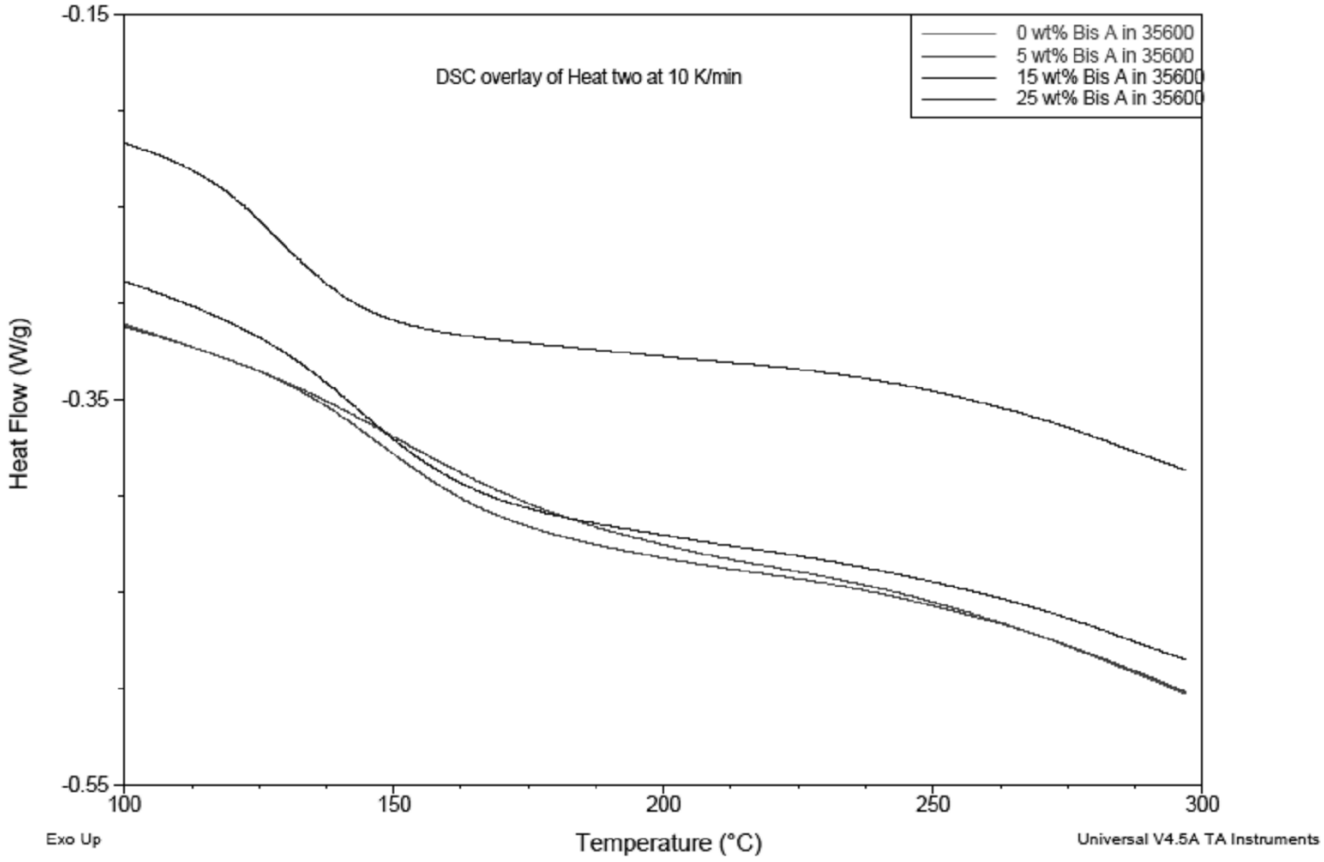

Fig. 6 DSC overlay of second heating scans for BA-a containing different concentrations of BPA.

In this case, the data are much easier to interpret (Table 4), although having been exposed to a full cure schedule, the values of T_g (determined from the peak maxima in the loss modulus data) are all significantly higher than the values derived from DSC, but aside from the lowest BPA content, a similar trend is observed.

Table 4 DMTA data for cured resin blends

Sample	T_g (°C)	$T_e = (T_g + 30\ K)$ (°C)	$3RT_e$	G_e (MPa)	ν (x 10^{-3} mol cm^{-3})
BP-a	183	213	5198	29.4	5.7
BA-a/$BPA_{5\%}$	185	215	5251	33.8	6.4
BA-a/$BPA_{15\%}$	166	196	4783	36.8	7.7
BA-a/$BPA_{25\%}$	148	178	4349	64.9	14.9

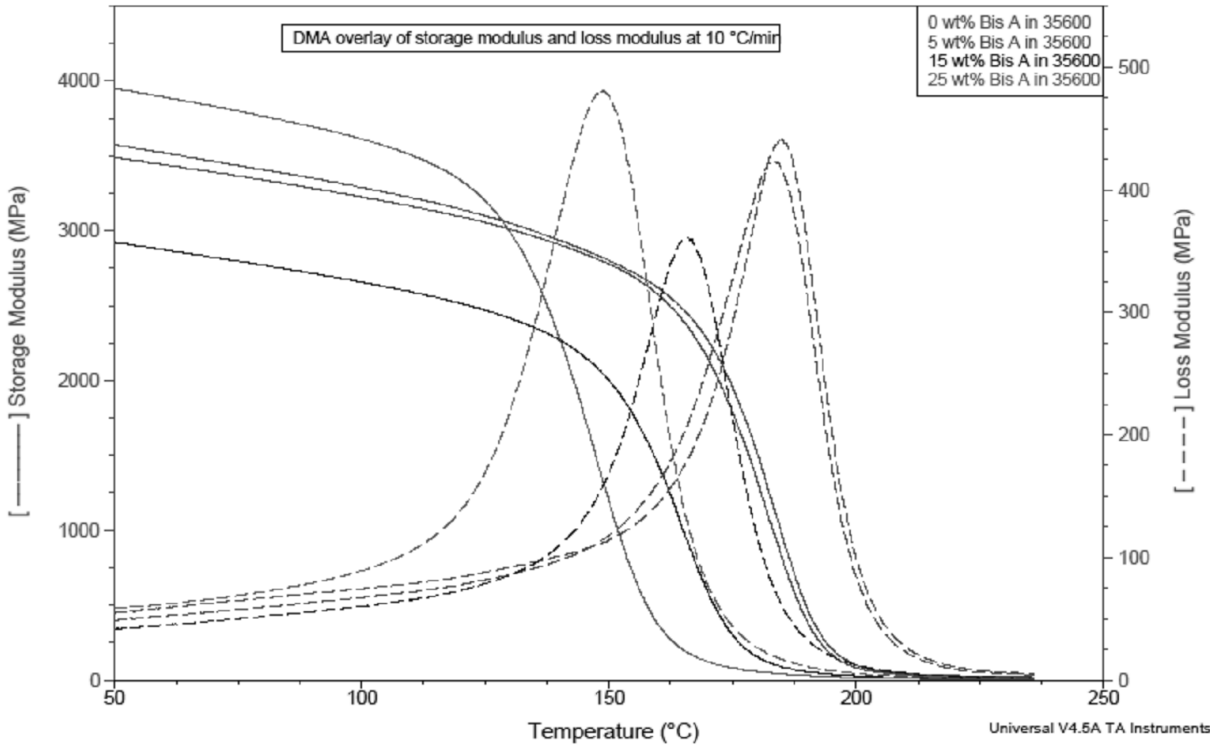

Fig. 7 DMTA overlay (10 K/min) for storage and loss modulus data for poly(BA-a) containing different concentrations of BPA.

The crosslink density (ν) for each of the cured polybenzoxazine networks was calculated from the DMTA data using (Eq. 1)[41]:

$$\nu = G_e/\varphi R T_e \qquad \text{(Eq. 1)}$$

Where φ is taken as 3, G_e is the storage modulus strictly from a sample at equilibrium, but is taken at T_e, where $T_e = (T_g + 30\ K)$, R = gas constant (8.314 J/K/mol.).

This equation is technically most appropriate for lightly cross-linked materials so it should only be used as a comparison between similar materials (*i.e.* in a homologous series), rather than giving a definitive value for crosslink density. This leads to a value of $\nu = 5.7$ mol m^{-3} for BA-a, which is in good agreement with previous reports for the polymer derived from this monomer**Error! Bookmark not defined.**. Typical values of crosslink density for a variety of polybenzoxazines have been reported[42,43,44,45] are 1.1-10.5 x 10^{-3} mol cm^{-3}. For the homologous series, as the T_g falls the crosslink density rises, to threefold that of the BA-a homopolymer. This somewhat paradoxical finding must reflect the differences in network structure that are being produced with the incorporation of BPA. Thus, the cross-link density cannot straightforwardly used to discuss the T_g as we do not know of the effect of cross-link density on the two chemically differing network

structures that coexist. On the other hand, the increased chain-flexibility (introduced through a greater concentration of ether linkages) becomes an important parameter to influence the T_g. Although little has been done to examine the effect of adding BPA to benzoxazine monomers, there are some precedents for their use in epoxy chemistry, where it is well known that BPA might act as both an initiator or a catalyst when co-reacted in the molten state with the corresponding diglycidyl ether. Pertinently, Smith and Ishida[46] found that the phenol and epoxide reaction was found to proceed to a level of 50 % at which point the phenolic species activated the branching reaction. A similar situation appears to take place here with BA-a blends containing lower BPA concentrations seeming to favour linear chain growth rather than branching with profound changes seen in both reactivity and final properties.

The cured BA-a/BPA blends were analysed as neat resin plaques using TGA under flowing nitrogen and the data are presented in Table 5. It is immediately apparent that BA-a and BA-a/$BPA_{5\%}$ display comparable thermal stability across the entire temperature range, but as the BPA is increased the stability of the cured copolymer is reduced, with the blend containing 25 wt % displaying markedly lower onset of thermal degradation (265 °C *cf* 289 °C for the homopolymer, poly(BA-a)) and lower char yield.

Table 5 Thermal stability of polymers in nitrogen (heating rate 10 K $min.^{-1}$, flow rate 60 cm^3 $min.^{-1}$).

Sample	Temperature (°C) at which mass loss was recorded					Y_c (%)
	5 %	10 %	20 %	25 %	50 %	
Poly(BA-a)	289	323	355	367	410	26
Poly(BA-a/$BPA_{5\%}$)	297	325	355	366	412	26
Poly(BA-a/$BPA_{15\%}$)	283	309	337	350	410	26
Poly(BA-a/$BPA_{25\%}$)	265	293	322	333	383	22

Key: Y_c = residual char remaining at 800 °C

The mechanism of degradation is similar in all blends, with the characteristic three steps visible in the derivative data[47,48], but as the BPA content is increased, the contribution of the first loss in mass (*ca.* 150-200 °C) becomes more marked. This is consistent with the view that the BPA is acting as a reactant forming BPA branches as the typical polybenzoxazine degradation thermogram has three major peaks, the lowest temperature of which is hypothesized to be due to the chain ends or branches[49] (Ishida *et al.* found that one molar equivalent of BPA yielded two molar equivalents of reactants). In the present work, while the oxazine group is consumed by homopolymerization and continues to reduce the number of oxazine molecules, the stoichiometry may shift to the extent that

too much of BPA is present for the higher content BPA samples, leading to more BPA side chains, that degrade at a relatively low temperature.

Examination of thermal transitions in cured polybenzoxazines using molecular simulation. Key to the success of molecular simulation of polymers is the construction of 'realistic' atomistic models of the polymer under consideration. We have developed an automatic method for generating models of cross linked polymers by linking reactive groups followed by energy minimisation and a short MD simulation to relax the structure to regularise the bond lengths formed. This process was described for epoxies in Howlin *et al.*[50]. The validity of these models is checked by simulating the models under MD at a range of temperatures to simulate T_g and T_d. The correct correlation of these parameters with experimentally determined values indicates that the network is behaving as expected by experiment. A series of simulated cured copolymers is shown in Fig. 9, from which it is immediately apparent that the network becomes less compact as the BPA content is increased, which is demonstrated by the lower degree of crosslinking (Table 6). Furthermore, during the construction of the polybenzoxazine networks, two cut-off distances were employed (0.5 nm and 0.6 nm) to yield cured networks with different crosslink densities. The longer the cut-off distance, the greater the number of atoms that might potentially undergo co-reaction and bond formation (and hence the higher the degree of polymerisation and crosslink density achieved).

Table 6 Automatically generated models using *in silico* cure programme at different cut off distances

Sample	Cut off distance (nm)	Number of BPA molecules	Number of BA-a monomers	Crosslinking (%)
Poly(BA-a)	0.5	0	70	111/140 = 79
	0.6	0	70	125/140 = 89
Poly(BA-a/$BPA_{5\%}$)	0.5	9	85	134/170 = 78
	0.6	9	85	149/170 = 87
Poly(BA-a/$BPA_{15\%}$)	0.5	27	75	112/150 = 74
	0.6	27	75	123/150 = 82
Poly(BA-a/$BPA_{25\%}$)	0.5	44	65	89/130 = 68
	0.6	44	65	102/130 = 78
Poly(BA-a/$BPA_{35\%}$)	0.5	71	65	86/130 = 66
	0.6	71	65	98/130 = 75

Following MD simulation the density of each model was monitored with respect to simulation temperature to discern significant changes in this parameter and relate it to structural changes taking place in the polymer. Two features were specifically targeted: the α and β transitions, relating to the temperature at which significant network translational movement and minor rotation/motion of branches or individual moieties.

The plots of simulated density *versus* temperature form the MD simulation for poly(BA-a) and poly(BA-a/$BPA_{5\%}$) are shown in Fig. 8, from which several features are apparent and which correlate well with empirical data (Table 7). At lower temperatures (25-40 °C), a small drop in the density is apparent. A second drop is also observed at 75-90 °C corresponding to the β transition observed in the DMTA data for this polymer (Fig. 7). This corresponds well with previously reported values of the β-transition of poly(BA-a) (70-80 C)[51].

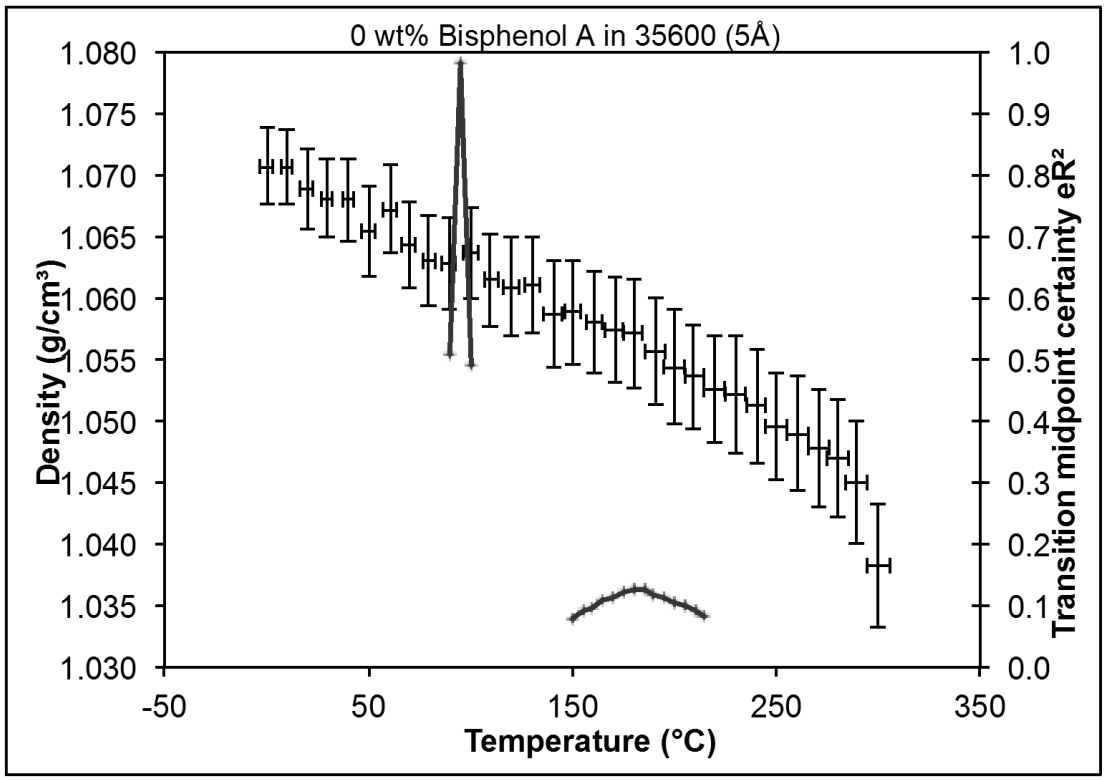

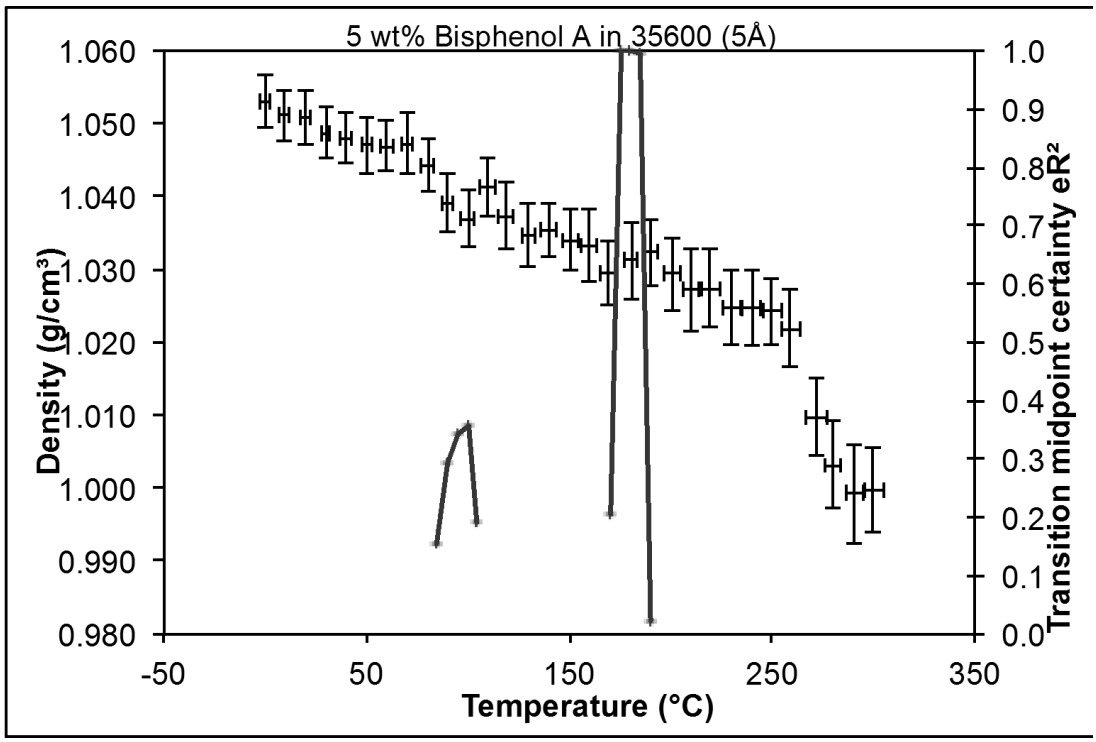

Fig. 8 Simulated density *versus* temperature for the poly(BA-a) model containing 0 wt % BPA (top) and 5 wt % BPA (bottom).

The glass transition (α transition) is also marked by the larger fall at 180-190 °C. The large drop in density at 280 °C may correspond to the thermal degradation of the polymer. The red transition midpoint certainty is used to locate the deviations in the data by fitting a jointed line with ellipses reflecting the standard deviations in both axes of the data and locating the maximum change in slope. This process is fully described in Howlin *et al.*[52]. Using this methodology, the glass transition temperatures for the different blends using empirical and simulation are compared in Table 6; in general the shorter cut off distance tends to be more consistent with the lower T_g produced using DSC, while the longer cut off is consistent with the DMTA data. Both data for BA-a were in agreement with the manufacturer's literature[53].

Table 7 Comparison of T_g determined from thermal analysis and molecular modelling

Sample	Empirical Data (°C)		Molecular Modelling (°C)	
	T_g (DSC)	T_g (DMTA)	T_g (cut off 0.5 nm)	T_g (cut off 0.6 nm)
Poly(BA-a)	180	180-190	180	190
Poly(BA-a/$BPA_{5\%}$)	170	180-190	180-190	190
Poly(BA-a/$BPA_{15\%}$)	150	160-170	150-160	160-170
Poly(BA-a/$BPA_{25\%}$)	120-130	140-150	130-140	140-150
Poly(BA-a/$BPA_{35\%}$)	115-125	-	120	125

The simulated values of T_g were in good agreement with thermal and dynamic mechanical data and although the brittle poly(BA-a/$BPA_{35\%}$) could not be tested, the MD simulation predicts a T_g of 120-125 °C for it (the lowest of the copolymers).

Examination of free volume in cured polybenzoxazines using molecular simulation. One model, poly(BA-a/$BPA_{5\%}$), was selected for a more detailed analysis of the influence of free volume on the thermal transitions observed. Two individual frames from the trajectory files were selected for comparison: the point at which the α and β transitions are indicated (Fig. 9, , see supplementary Fig. S3 for coloured images). Three principal differences between the models were observed: the smallest circle shows the phenyl ring, which extends by a quarter out of the PBC cell at 373 K. As the temperature decreases, the ring extends further to one half. In the largest circled region (showing an oxazine ring), as the temperature is reduced the ring and the main backbone become rotated towards the front of the cell. The intermediately sized circled region (the nitrogen atom forming the oxazine ring) were extended beyond the cell at 453 K, but contained within it at 373 K.

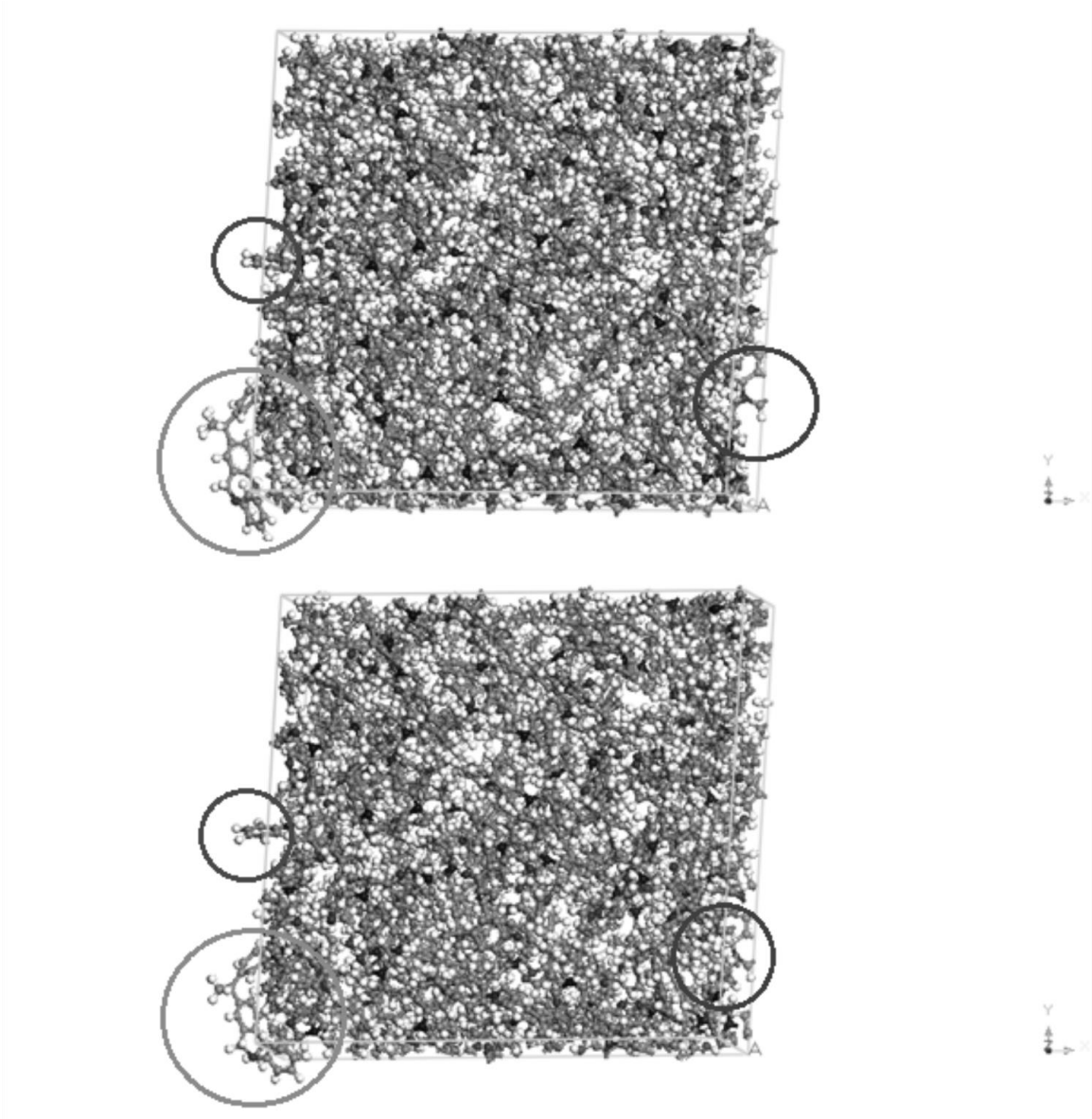

Fig. 9 Atomistic model of poly(BA-a/$BPA_{5\%}$) (0.5 nm cutoff distance). Top cell: frame of atomistic model at 453 K (180 °C); bottom cell: frame of atomistic model at 373 K (95-100 °C).

In parallel, an examination of the solvent accessible surface area was performed on both examples of this model (*i.e.* using the same frames described above, at the α and β transitions). The simplest way to simulate the accessible volume (and thus potentially the moisture uptake in these systems) is to look at the solvent accessible free volume in the models. This is calculated from the Connolly surface[52] with a probe radius of 0.14 nm representing a water molecule (Fig. 10, see supplementary Fig. S4 for coloured images). Water molecules were packed into this accessible free volume until no more would fit and the occupied volume (and hence the free volume) calculated (Table 8).

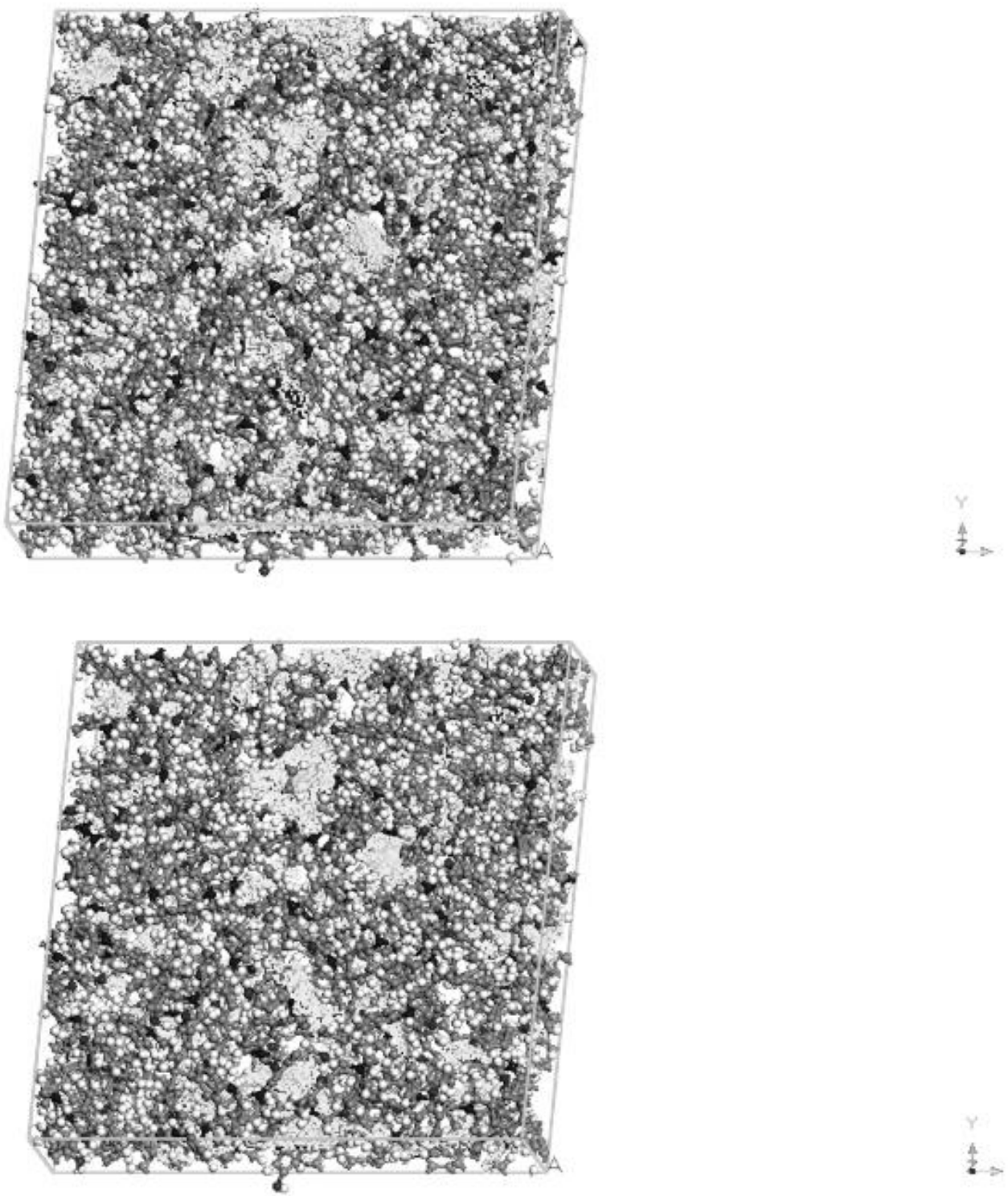

Fig. 10 Solvent accessible free volume (shaded surface) in poly(BA-a/BPA$_{5\%}$) (0.5 nm cut off distance) at (a) 453 K (180 °C) and (b) 373 K (95-100 °C).

Table 8 Simulated available solvent-accessible surface area calculated for Poly(BA-a/$BPA_{5\%}$) using different *in-silico* cure conditions

'Cure' conditions	Occupied volume (nm^3)	Free volume (nm^3)	Free volume (%)
0.5 nm at 453 K	6719	919	1.4
0.5 nm at 373 K	6657	931	1.4
0.6 nm at 463 K	6596	850	1.3
0.6 nm at 373 K	6599	758	1.2

CONCLUSIONS

The introduction of comparatively modest amounts of bisphenol A can lead to a significant reduction in the polymerisation temperature of a benzoxazine monomer, with comparable glass transition temperature and superior thermal stability to the cured commercial polymer. Further increase of T_g can be observed as the content of bisphenol A in the blend increases, but at the expense of physical and mechanical properties. The simulation of these copolymeric networks yields thermal events (α and β transitions) that are in good agreement with empirical data obtained using DSC and DMTA.

ACKNOWLEDGEMENTS

We thank The Majlis Amanah Rakyat (MARA) for funding (WAWH) in the form of a studentship. We thank Huntsman Advanced Materials (Basel, Switzerland) for supplying the benzoxazine monomer.

REFERENCES

(1) Ishida, H.; Ohba, O. *Polymer* **2005**, *46*, 5588-5595.

(2) Sudo, A.; Kudo, R.; Nakayama, H; Arima, K.; Endo, T. *Macromolecules* **2008**, *41*, 9030-9034.

(3) Ishida, H.; Rodriguez, Y. *J. Appl. Polym. Sci.* **1995**, *58*, 1751-1760.

(4) Ning, X.; Ishida, H.J. *J. Polym. Sci. – Polym. Phys.* **1994**, *32*, 921-927.

(5) Ishida, H.; Rodriguez, Y. *Polymer* **1995**, *36*, 3151-3158.

(6) Russel, V.; Koenig, J.L.; Low, H.Y.; Ishida, H. *J. Appl. Polym. Sci.* **1998**, *70*, 1401-1411.

(7) Russel, V.; Koenig, J.L.; Low, H.Y.; Ishida, H. *J. Appl. Polym. Sci.* **1998**, *70*, 1413-1425.

(8) Jang, J.S.; Shin, S.H. *Polymer J.* **1995**, *27*, 601-605.

(9) Yu, D.S.; Chen, H.; Shi, Z.; Xu, R. *Polymer* **2002**, *43*, 3163-3168.

(10) *Handbook of Polybenzoxazine Resins*, H. Ishida; T. Agag (Eds.) Elsevier: New York, 2011, p. 9.

(11) Nielsen, L.M. *Mechanical Properties of Polymers and Composites*, Marcel Dekker: New York, **1974**, pp. 174-181.

(12) Ishida, H.; Lee, Y.H. *J. Appl. Polym. Sci.* **2001**, *81*, 1021-1934.

(13) Lu, H.; Zheng, S. *Polymer* **2003**, *44*, 4689-4698.

(14) Ishida, H.; Lee, Y.H. *Polymer* **2001**, *42*, 6971-6979.

(15) Ishida, H.; Lee, Y.H. *J. Polym. Sci. Polym. Phys.* **2001**, *39*, 736-749.

(16) Zheng, S.; Lu, H.; Guo, Q. *Macromol. Chem. Phys.* **2004**, *205*, 1547-1558.

(17) Kimura, H.; Matsumoto, A.; Hasegawa, K.; Ohtsuka, K.; Fukuda, A. *J. Appl. Polym. Sci.* **1998**, *68*, 1903-1910.

(18) Rao, B.S.; Rajavardhana, K.R.; Pathak, S.K.; Pasala, A.R. *Polym. Internat.* **2005**, *54*, 1371-1376.

(19)http://henkelna.com/us/content_data/232113_Benzoxazine_Matrix_Resins_for_Structural_Composite_Applications.pdf (accessed 21st October, 2015).

(20) Rimdusit, S.; Ishida, H. *Polymer* **2000**, *41*, 7941-7949.

(21) Rimdusit, S.; Ishida, H. *Rheol. Acta* **2002**, *41*, 1-9.

(22) Rimdusit, S.; Ishida, H. *J. Polym. Sci.* **2000**, *38*, 1687-1698.

(23) Kimura, H.; Taguchi, S.; Matsumoto, A.*J. Appl. Polym. Sci.* **2001**, *79*, 2331-2339.

(24) Culbertson, B.M.; Tiba, O.; Deviney, M.L.; Tufts, T.A. *SAMPE* **1989**, *34*, 2483.

(25) Agag, T.; Takeichi, T. *Mater. Sci. Forum* **2004**, *449-452*, 1157-1160.

(26) Agag, T.; Takeichi, T. *Polymer* **2000**, *41*, 7083-7090.

(27) Shi, Z.; Yu, D.S.; Wang, Y.; Xu, R. *Eur. Polym. J.* **2002**, *38*, 727-733.

(28) Shi, Z.; Yu, D.S.; Wang, Y.; Xu, R. *J. Appl. Polym. Sci.* **2003**, *88*, 194-200.

(29) Takeichi, T.; Zeidam, R.; Agag, T. *Polymer* **2002**, *43*, 45-53.

(30) Unscrambler X v10.1, **2011**, Camo Software, Inc., USA.

(31) Materials Studio v6.0.0.0, **2012**, Accelrys Inc., San Diego, USA.

(32) Sun, H.; Mumby, S.J.; Maple, J.R.; Hagler, A.T. *J. Amer. Chem. Soc.* **1994**, *116*, 2978-2987.

(33) Burkert, U.; Allinger, N.L. *Molecular Mechanics*, ACS Monograph, **1982**, p. 177.

(34) Goodman, J.M. *Chemical Applications of Molecular Modelling*, RSC: Cambridge, **1998**, pp. 31-60.

(35) Allen, F.H.; Watson, D.G.; Brammer, L.; Opren, A.G.; Taylor, R. Typical interatomic distances: organic compounds, in *International Tables for Crystallography* **2006**, pp. 790-811.

(36) Liu, X.; Gu, Y. *Sci. China* **2001**, *44*, 552-560.

(37) Jang, J.S.; Yang, H. *Comp. Sci. Tech.* **2000**, *60*, 457-463.

(38) Jang, J.S.; Seo, D. *J. Appl. Polym. Sci.* **1998**, *67*, 1-10.

(39) Hamerton, I.; Douse, E.; Kopsidas, S.; Jesson, D. Modification of stress-strain behaviour in aromatic polybenzoxazines using core shell rubbers, **2015**, submitted.

(40) Hamerton, I.; McNamara, L.T.; Howlin, B.J.; Smith, P.A.; Cross, P.; Ward, S. *Macromolecules* **2013**, *46*, 5117–5132.

(41) Grishchuk, S.; Mbhele, Z.; Schmitt, S.; Karger-Kocsis, J. *eXPRESS Polym. Lett*. **2011**, *5*, 273-282.

(42) Ishida, H.; Allen, D.J. *J. Polym. Sci., Part B: Polym. Phys.* **1996**, *34*, 1019-1030.

(43) Wang, Y.-X.; Ishida, H. *Polymer* **1999**, *40*, 4563-4570.

(44) Shen, S.B.; Ishida, H. *J. Polym. Sci., Part B: Polym. Phys.* **1999**, *37*, 3257-3268.

(45) Wang, Y.-X.; Ishida, H. *J. Appl. Polym. Sci.* **2002**, *86*, 2953-2966.

(46) Smith, M.E.; Ishida, H. *Macromolecules* **1994**, *27*, 2701-2707.

(47) Jayamohan Das, L.; Rajeev, R.; Rajeev, R. S.; Santhosh Kumar, K. S. *Int. J. Sci. Technol. Res.* **2013**, *2*, 146-155.

(48) Hamerton, I.; Thompson, S.; Howlin, B.J.; Stone, C.A. *Macromolecules* **2013**, *46*, 7605-7615

(49) Chernykh, A.; Liu, J.P.; Ishida, H. *Polymer* **2006**, *47*, 7664-7669.

(50) Hall, S.A.; Howlin, B.J.;Hamerton, I.; Baidak, A.;Billaud, C., Ward, S. PLOSone, 2012, DOI: 10.1371/journal.pone.0042928.

(51) Rimdusit, S.; Punson, K.; Dueramae, I.; Somwangthanaroj, A.; Tiptipakorn, S. *Eng. J.* **2011**, *15*, Thailand, 15, may. 2011. Available at: <http://engj.org/index.php/ej/article/view/147/92>. Date accessed: 24 Aug. 2015.

(52) Conolly, M.L. *J. Appl. Cryst*. **1983**, *16*, 548-558.

(53) http://www.maxepoxi.com.br/pdf/sortimento_araldite_benzoxazines.pdf, Huntsman Corporation, accessed 02/12/2013.